Journal of
Clinical & Translational Ophthalmology

MDPI

Review

Ophthalmic Imaging in Diabetic Retinopathy and Diabetic Macular Edema: Key Findings and Advancements

Akanksha Malepati [1], Edmund Arthur [2] and Maria B. Grant [1,3,*]

[1] UAB Heersink School of Medicine, University of Alabama at Birmingham, Birmingham, AL 35294, USA; amalepat@uab.edu
[2] School of Optometry, University of Alabama at Birmingham, Birmingham, AL 35294, USA; earthur@uab.edu
[3] Department of Ophthalmology and Visual Sciences, University of Alabama at Birmingham, Birmingham, AL 35294, USA
* Correspondence: mariagrant@uabmc.edu; Tel.: +1-352-871-4314

Abstract

Diabetes mellitus (DM) is a debilitating chronic disorder that results in ocular microvascular complications, including diabetic retinopathy (DR) and diabetic macular edema (DME). Early detection and timely intervention for DR and DME are crucial for improving visual outcomes in affected patients. Ophthalmic imaging plays a vital role in the screening, diagnosis, and management of DR and DME. In this review, a comprehensive overview of the imaging modalities frequently utilized in the assessment of DR and DME, encompassing both structural and functional imaging techniques are presented. The key imaging findings that are associated with the various stages of DR and DME are underscored and their diagnostic utility in assessing disease progression and visual function are evaluated. Additionally, we discuss emerging imaging biomarkers that are currently under investigation, which hold significant potential for improving the diagnostic and prognostic capabilities of imaging for DR and DME patients. Finally, the advent of new imaging methods, such as ultrawide-field imaging (UWFI) and deep learning models, which have markedly improved the detection of retinal pathologies are considered.

Keywords: diabetic macular edema; imaging; spectral domain optical coherence tomography; optical coherence tomography angiography; fluorescein angiography; color fundus photography; fundus autofluorescence

check for updates

Academic Editor: Thomas Desmettre

Received: 28 June 2025
Revised: 3 October 2025
Accepted: 5 November 2025
Published: 7 November 2025

Citation: Malepati, A.; Arthur, E.; Grant, M.B. Ophthalmic Imaging in Diabetic Retinopathy and Diabetic Macular Edema: Key Findings and Advancements. *J. Clin. Transl. Ophthalmol.* **2025**, *3*, 24. https://doi.org/10.3390/jcto3040024

Copyright: © 2025 by the authors. Licensee MDPI, Basel, Switzerland. This article is an open access article distributed under the terms and conditions of the Creative Commons Attribution (CC BY) license (https://creativecommons.org/licenses/by/4.0/).

1. Overview of Diabetic Retinopathy (DR) and Diabetic Macular Edema (DME)

Diabetes mellitus (DM) is a chronic metabolic disorder characterized by persistent hyperglycemia, currently affecting 11.6% of the United States (US) population [1]. DM results in several macrovascular and microvascular complications, including stroke, coronary artery disease, diabetic kidney disease, peripheral neuropathy, and retinopathy [2].

Diabetic retinopathy (DR) is a microvascular ocular complication of DM that results from prolonged hyperglycemia, leading to vascular endothelial dysfunction, retinal inflammation, and retinal neurodegeneration. DR can be classified into two main subcategories: non-proliferative diabetic retinopathy (NPDR) and proliferative diabetic retinopathy (PDR) (Figure 1). NPDR is further divided into mild, moderate, and severe stages depending on the degree of retinal microvascular damage (Figure 1). Conversely, PDR is characterized by the development of neovascularization and aberrant blood vessels, which arise in response to retinal ischemia [3] (Figure 1). Diabetic macular edema (DME), which can occur at any

stage of DR, arises from weakened vessel walls and breakdown of the blood–retinal barrier, leading to fluid leakage and subsequent fluid accumulation in the macula [4]. Figure 1 shows the progression of DR, as classified by the Early Treatment Diabetic Retinopathy Study (ETDRS).

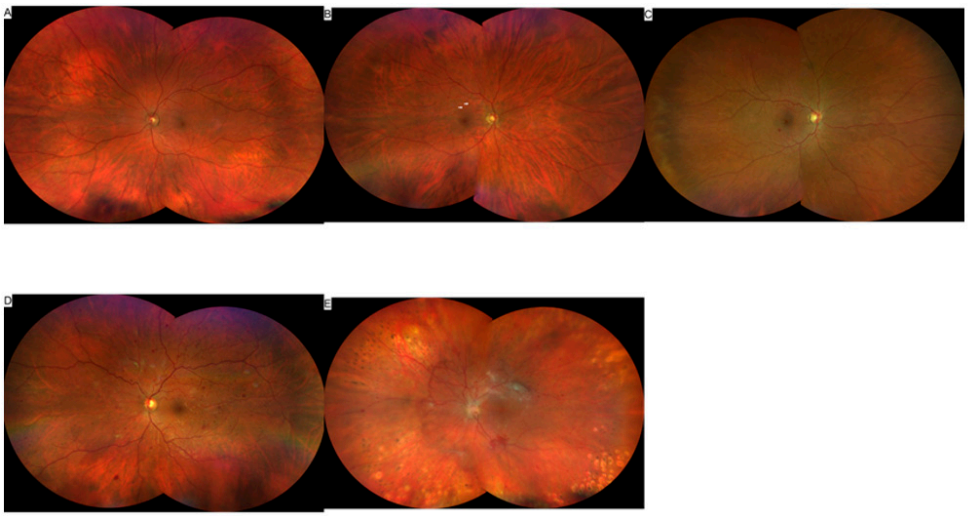


Figure 1. Color fundus images showing the Early Treatment Diabetic Retinopathy Study (ETDRS) grading of DR. (**A**) no DR, (**B**) mild NPDR, arrows show dot and blot hemorrhages, (**C**) moderate NPDR, (**D**) severe NPDR, and (**E**) PDR.

Notably, DR ranks as the fifth leading cause of blindness globally, and its prevalence is expected to rise in parallel with the global burden of DM [5]. Therefore, ophthalmic imaging in DR and DME patients is essential for diagnostic purposes and for managing the progression of disease promptly to prevent worsening of visual outcomes in affected patients [6]. There are several imaging techniques that can be used to characterize the severity of DR and DME. These include, but are not limited to, Spectral Domain Optical Coherence Tomography (SD-OCT), Optical Coherence Tomography Angiography (OCT-A), Fluorescein Angiography (FA), Color Fundus Photography (CFP), and Fundus Autofluorescence (FAF), which will be the focus of this review.

2. Structural Retinal Imaging Techniques

2.1. Color Fundus Photography (CFP)

CFP is a valuable structural imaging tool that provides insight into retinal vascular pathology in DR and DME [7]. New fundus cameras can provide an expanded field of view up to 55°, enabling an image of the macula and optic nerve in a single frame. This is a significant improvement over older cameras that only provided a 30° field of view [8]. The most commonly used grading system for DR and DME is the Diabetic Retinopathy Severity Scale (DRSS), which was derived from the Early Treatment Diabetic Retinopathy Study (ETDRS) grading scale. ETDRS utilizes seven standard retinal fields consisting of stereoscopic 30° color photographs [9]. These images capture approximately 30% of the retinal surface and show the macula, optic nerve, and vascular arcades [9,10]. Initially, based on an examination of the standard 7 fields, the ETDRS scale consists of 13 levels that range from the absence of DR to severe PDR, which is characterized by advanced PDR with either the detachment of the macula or obscured posterior fundus [11,12]. This scale was distilled into the current DRSS scale, which consists of five stages that correlate to the ETDRS for ease of use in clinical settings and general DR assessment: no visible retinopathy, mild NPDR, moderate NPDR, severe NPDR, and PDR, with DME having the ability to present at any level [13].

CFP findings in DR and DME images are utilized to grade patients on the ETDRS and DRSS scale. In standard 30° 7-field CFP images, the presence and grade of fundus lesions such as hemorrhages, microaneurysms, hard exudates, soft exudates cotton wool spots, venous beading and loops, intraretinal microvascular abnormalities (IRMAs), neovascularization, arteriovenous nicking, retinal elevation, and vitreous hemorrhage are used in the characterization of DR [12]. Mild NPDR is characterized by at least one microaneurysm present, with no signs of moderate NPDR. Moderate NPDR requires the presence of any of the following: microaneurysms, retinal or dot blot hemorrhages, and hard or soft exudates, with no signs of severe NPDR. Severe NPDR has more than twenty intraretinal hemorrhages in all four quadrants, venous beading in at least two quadrants, and prominent IRMA in at least one quadrant, with no signs of PDR; this is referred to as the 4-2-1 rule. PDR requires neovascularization, vitreal hemorrhage/preretinal hemorrhage, or the presence of both. Finally, DME is characterized by apparent thickening or exudates within one disc diameter of the fovea [10,14].

Despite the extensive use of CFP in the imaging of DR and DME, CFP presents with a set of notable limitations. Apart from the necessity for mydriasis in order to obtain an appropriate image, CFP is also constrained by low image quality in the presence of media opacities and inherent two-dimensional images [15]. Additionally, CFP has a restricted field of view, failing to capture approximately 70% of the retinal surface in the standard 7-field view [15]. Consequently, DR severity in some patients may be misdiagnosed as a result of imaging missing peripheral lesions. The use of ultrawide-field imaging (UWFI) is currently being investigated to address this limitation. Several studies have demonstrated that 10% to 20% of patients assessed with UWFI exhibit a greater severity of DR in comparison to those evaluated with the ETDRS standard 7-field imaging [16–18]. Indeed, one study showed that though less than 5% of a cohort of patients displayed a difference in their DR severity when assessed with the ETDRS standard 7-field compared to UWFI, significant vision-threatening lesions, such as neovascularization and preretinal hemorrhages, were detected in the peripheral regions outside the standard 7-fields [19]. Indeed, another study comparing ETDRS standard 7-field imaging compared to UWFI found that peripheral lesions detected on UWFI led to a two-step or greater increase in ETDRS DR severity in 11% of cases [16]. Therefore, UWFI (Figure 2) has the potential to provide a more comprehensive assessment of DR and DME severity, thus leading to more accurate diagnoses that can guide management and treatment.



Figure 2. Severe Non-Proliferative Diabetic Retinopathy (NPDR). A montage image of an eye with NPDR was created from two widefield (133°) images, yielding an ultra-widefield (UWF) view. Color

fundus photograph of the left eye (OS) from a 43-year-old white male with severe NPDR. The image displays several hallmark features of advanced disease, including: Numerous dot and blot hemorrhages scattered across all four retinal quadrants. Significant venous beading, giving the retinal veins a characteristic "string of sausages" appearance. Areas of intraretinal microvascular abnormalities (IRMA), representing dilated and tortuous intraretinal capillaries. The image was obtained using the Zeiss Clarus 500 (Carl Zeiss Meditec, Dublin, CA, USA). The combination of these findings, particularly hemorrhages in four quadrants and venous beading, classifies the retinopathy as severe and places the patient at a high risk for progression to proliferative disease.

2.2. Spectral-Domain Optical Coherence Tomography (SD-OCT)

SD-OCT is a non-invasive structural imaging tool that provides high-resolution cross-sectional images of the retina and choroid. SD-OCT is the gold standard for detecting DME, as it is highly sensitive and reproducible. A number of DME-specific findings are highlighted on SD-OCT [20].

As shown in Figure 3, disorganization of retinal inner layers (DRIL) is a reliable surrogate DME finding that is used to assess visual acuity in patients with current or resolved DME. DRIL is defined as an inability to differentiate between the ganglion cell layer, inner plexiform layer, and outer nuclear plexiform layer (Figure 2). DRIL is measured by assessing OCT B-scans of the central 1-mm-wide foveolar zone. If DRIL affects more than 50% of this zone, it is associated with worse visual outcomes [21]. DRIL has also been correlated with the progression of DR to later stages, specifically to PDR [22], disrupted external limiting membrane and ellipsoid zone [23], macular capillary non-perfusion [24], Müller cell dysfunction [25], and greater foveal avascular zone (FAZ) area [26]. Therefore, DRIL is a valuable marker for perfusion status and visual acuity, especially when assessing clinical treatments [27].

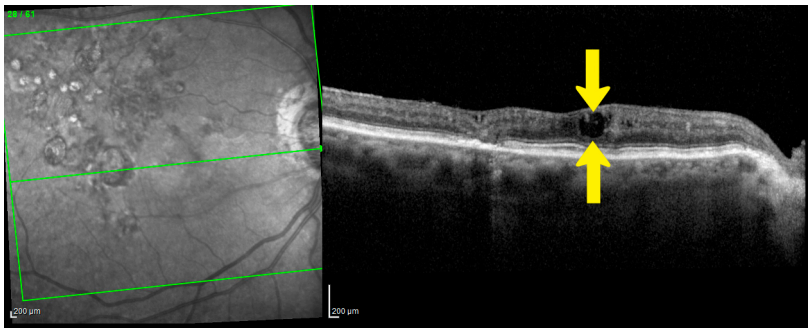


Figure 3. Disorganization of Retinal Inner Layers (DRIL) as an Early Indicator of Neurodegeneration. Spectral Domain-OCT (SD-OCT) B-scan of the right eye (OD) from a 86-year-old female patient with Diabetic Macular Edema (DME). The image demonstrates significant DRIL (area between yellow arrows), where the normal distinct boundaries between the inner retinal layers are lost. This structural disorganization is a biomarker for neurodegeneration and is considered the beginning of irreversible neural damage, making it a key prognostic indicator for poor long-term visual acuity. Image was obtained with Spectralis HRA + OCT (Heidelberg Engineering, Heidelberg, Germany). Green lines show the scan area on the infra-red fundus image.

Hard exudates are one of the most common lesions found on SD-OCT in DR [28]. Hard exudates are lipoprotein exudates that appear as hyperreflective areas larger than 30 µm in the inner and outer nuclear layer and outer plexiform layer, with back-shadowing due to breakdown of the inner-BRB [27–29]. Recent research has shown that, in contrast with small hyperreflective foci (HRF), which are inflammatory in origin, larger HRF corresponds to hard exudates (Figure 4) [30]. Increased total hard exudate area correlates with elevated triglyceride levels, which are, in turn, linked to greater central macular

involvement in DME [31]. Advancements in deep learning models have demonstrated accurate detection of hard exudates and DRIL in retinal imaging, with high sensitivity and specificity [32]. Overall, monitoring the size and distribution of hard exudates over time can provide valuable insights into the progression of DME and treatment effectiveness. HRF are small, distinct spots. HRF are small, dot-like lesions seen across all retinal layers on spectral-domain or swept-source OCT that are more reflective than the retinal pigment epithelium band [20]. They are typically less than 30 microns in size, lacking back-shadowing not visible on fundus photography. In DME, HRF are thought to represent activated microglial cells responding to ischemia and inflammation and lipid-laden macrophages, potentially precursors to hard exudates. HRF density correlates with levels of CD14, a macrophage/microglial marker, reinforcing their inflammatory origin [33].

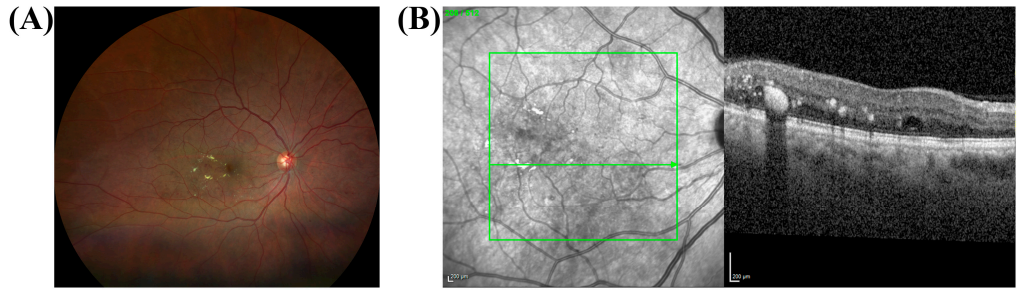


Figure 4. Hard Exudates and their OCT Correlates in a 63-year-old African American female with moderate non-proliferative diabetic retinopathy (NPDR) and diabetic macular edema (DME). (**A**) Color fundus photograph of the right eye (OD) shows hard exudates (yellow deposits) and scattered microaneurysms (small red dots). (**B**) The corresponding SD-OCT scan reveals hyperreflective foci (HRF), which are the structural correlates of DR lesions. The green line indicates the location of the spectral-domain OCT scan shown in (**B**). The larger, well-defined HRF corresponds directly to the hard exudates seen in the fundus photo (**A**). These larger foci are primarily located in the outer plexiform layer and cast a distinct shadow on deeper retinal layers. The scan also shows evidence of DME, which is characterized by retinal thickening and intraretinal fluid, consistent with the patient's condition. The color fundus and OCT images were obtained with Zeiss Clarus 500 (Carl Zeiss Meditec, Dublin, CA, USA) and Spectralis HRA + OCT (Heidelberg Engineering, Heidelberg, Germany), respectively. Green lines in (**B**) show the scan area on the infra-red fundus image.

In cases where retinopathy is undetectable, HRF are detected in diabetic eyes and increase in quantity as DR progresses [34]. In DME patients who had HRF in the outer retinal layers compared to those without, the logarithm of minimal angle of resolution visual acuity (logMAR VA) was significantly lower, and both the external limiting membrane and junction between the inner and outer segments were more significantly disrupted [35]. HRF may serve as a proxy for microglial activation, as they initially emerge in the inner retina where resident microglia are located and subsequently progress to the outer retinal layer [34]; this is further supported by a strong correlation between soluble CD14 (sCD14), a cytokine that is released by retinal macrophages and microglia, and the number of HRF, thus suggesting that HRF on SD-OCT represents activated microglia in the context of DME [33]. Indeed, the efficacy of various treatments for DME, including dexamethasone, intravitreal bevacizumab, aflibercept, and anti-VEGF, has been assessed via quantification of HRF using SD-OCT [36]. Though HRF quantification has been used to track treatment outcomes in DME, more work must be done to establish it as a standardized tool since its predictive value in the setting of visual outcomes is still debated [20].

Hyperreflective choroidal foci (HCF) are similar to HRF but are present in the choroid due to the hypothesized outward migration of HRF following disruption of the external limiting membrane and ellipsoid zone. The presence of HCF is associated with poor visual acuity in DME patients [37]. Furthermore, the presence of HCF is associated with worse vi-

sual acuity compared to eyes with solely HRF, though this difference was not significant [38]. Therefore, it is highly likely that HCF and HRF are pathophysiologically identical.

Another hallmark finding of DME is hyporeflective spaces within the retinal layers known as intraretinal cystoid spaces (Figure 5) [27]. These occur due to increased permeability of the iBRB, thus leading to extracellular fluid extravasation and cyst formation. During the initial stages of DME, solely the inner nuclear layer (INL) is affected, but later stages of DME are characterized by cystoid spaces in the outer plexiform layer (OPL) as well [39]. It has been suspected that intraretinal cysts in DME originate from the failure of Müller cells to remove fluid and subsequent liquefactive necrosis, though the development of OCT-A indicates that the deep vascular plexus may play a more significant role in fluid removal [40]. These intraretinal cystoid spaces are associated with vision loss and photoreceptor damage [27,41]. Large cysts, which are defined as larger than 220 µm, and outer nuclear layer (ONL) cysts have the most significant negative impact on retinal function when compared to smaller cysts and those in the INL [42]. Increased size of cysts and damage to the outer retinal layer were associated with increased likelihood for macular ischemia [43]. Furthermore, cysts in the outer layer of the retina damage photoreceptors beneath the cystoid space and disrupt the ellipsoid zone, thus leading to decreased visual function [27,44].

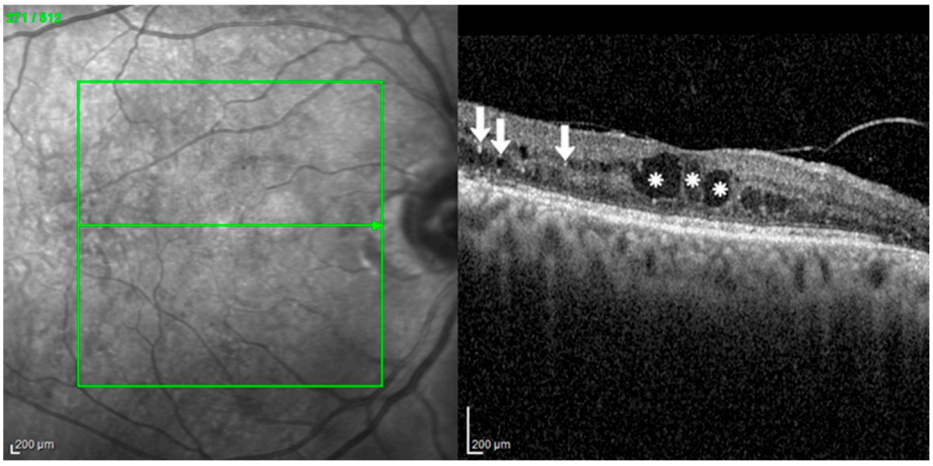


Figure 5. Intraretinal Cystoid Spaces and Hyperreflective Foci in Diabetic Macular Edema (DME). A spectral-domain OCT (SD-OCT) scan from a 60-year-old female with severe non-proliferative diabetic retinopathy (NPDR) and DME. Her visual acuity was 0.4 logMAR. The scan demonstrates classic findings of DME, including large intraretinal cystoid spaces (white asterisks), which are hyporeflective areas of fluid accumulation causing significant macular thickening. Additionally, numerous hyperreflective foci (HRF) (white arrows) are scattered throughout the retinal layers, signaling a prominent inflammatory component. The structural disruption from these features corresponds with the patient's reduced visual acuity. Image was obtained with the HRA + OCT (Heidelberg Engineering, Heidelberg, Germany). Green lines show the scan area on the infra-red fundus image.

Central subfield thickness (CSFT) and central retinal thickness (CRT) are quantitative measurements used in SD-OCT. CSFT is significantly increased in patients with clinically significant macular edema [45]. The increased permeability of the BRB in DME leads to the buildup of fluid in the subretinal and intraretinal areas, thus leading to this increased retinal thickness [46]. A CSFT that is greater than 250 µm has been used to indicate the presence of DME in recent clinical trials [47]. Therefore, CSFT is a useful diagnostic tool in DME. However, when assessing visual outcomes of patients with DME, CSFT should not be the sole biomarker that is used, as only a moderate, highly variable relationship has been established between these two variables [48]. There are several variables related to

CSFT that are being studied as new biomarkers. Recently, retinal thickness deviation has been shown to predict visual outcomes in DME patients undergoing intravitreal treatment more accurately than CRT/CSFT. Retinal thickness deviation, which was defined as the absolute value of the difference between measured retinal thickness and normative retinal thickness, was significantly positively correlated with best-corrected visual acuity [49]. Additional biomarkers that are associated with visual outcomes are DME pattern [39], quantified central macular fluid volume [50,51], extent of CSFT fluctuations [52], with larger fluctuations yielding worse visual acuity, extent of structural retinal damage [53], and quantified area of retinal tissue between plexiform layers [27]. Overall, these novel quantitative parameters related to CSFT could be used as a method to examine the efficacy of therapeutics in improving vision in DME patients.

The external limiting membrane (ELM), which consists of junctional complexes between photoreceptors and Müller cells and separates layers of rods and cones, corresponds to the first, innermost hyperreflective band on SD-OCT [54]. The ellipsoid zone (EZ) corresponds to the second hyperreflective band on SD-OCT and represents the ellipsoid portion of the inner photoreceptor segments [54]. Initially, there was some debate that the EZ corresponded to the boundary between the inner and outer photoreceptor segments, which is why the original terminology referred to the EZ by the term IS/OS junction [55]. Within the ELM, tight junctions composed of occludin, a transmembrane protein, prevent increased vascular permeability. VEGF alters these tight junctions via phosphorylation and ubiquitination, thus contributing to the pathogenesis of DME [56]. Conversely, the EZ reflects photoreceptor structure and function [57]. The disruption and integrity of the ELM and EZ are prognostic biomarkers of DME [58]. Disruption of the ELM and EZ has been proposed to be graded in three stages, with grade zero indicating no disruption of ELM or EZ, grade one being solely ELM disruption with the EZ intact, and grade two indicating both ELM and EZ disruption. Additionally, the integrity of the EZ is graded in three stages as well: grade zero indicates intact EZ, grade one represents focal, subfoveal EZ disruption, and grade two indicates global EZ disruption that involves the macular cube [59]. Both disruption and decreased integrity of the ELM and EZ are predictors of worse visual acuity in DME patients [60]. Therefore, evaluation of EZ and ELM disruption and integrity on SD-OCT is essential to the diagnosis and management of DME.

Vitreomacular interface abnormalities (VMIA) are defined by findings of epiretinal membrane (ERM), vitreomacular traction, posterior hyaloid traction, and posterior vitreomacular separation observed on SD-OCT. VMIA, specifically ERM and posterior vitreomacular separation, were found in 25% of a cohort of patients using SD-OCT [61], with up to 38% being reported in other studies [62]. VMIA are associated with poor visual outcomes and worsened DME [63,64]. Indeed, relief of vitreomacular traction has the potential to resolve DME in certain cases [65]. Additionally, VMIA abnormalities in DME patients significantly decrease the effectiveness of intravitreal anti-VEGF therapies [66]. Taken together, the assessment of VMIA provides a valuable tool for monitoring DME progression, visual function, and treatment outcomes.

2.3. Fundus Autofluorescence (FAF)

Autofluorescence occurs when a substrate known as a fluorophore is excited by a certain wavelength of light and emits a wavelength of light in return [67]. Fluorophores can either be endogenous, as in the case of FAF, where they are located in the retinal pigment epithelium (RPE), or exogenous, as in the case of FA, where a dye is injected [68]. The major fluorophore located in the retina is lipofuscin, which is an aging pigment located intracellularly as a result of the incomplete oxidative breakdown of photoreceptor outer segments that accumulate in lysosomes [69]. Specifically, N-retinylidene-N-retinylethanolamine

(A2E) is the major fluorophore component of lipofuscin, though additional components include other bisretinoids [69,70]. Lipofuscin has an emission spectrum in the yellow-orange region in response to excitation by ultraviolet and blue visible light [71]. As age increases and lipofuscin accumulates, the short-wavelength FAF (SW-FAF) signal intensity increases [71]. FAF is useful to investigate RPE stress (hyperautofluorescence) as lipofuscin is assumed to accumulate due to oxidative damage [68] and the hypoautofluorescence is a useful marker of RPE death [72–74].

Although lipofuscin accumulation in the RPE is characteristic of other retinal diseases, it has been hypothesized that in DME, lipofuscin granules accumulate in activated retinal microglia, which leads to increased FAF pattern areas [75]. Because normal patients have absent FAF in the foveola, increased FAF in DME patients is also hypothesized to represent damage to cone photoreceptors [76–78]. The prolonged increased FAF in patients following DME resolution results from retinal and photoreceptor cells capturing macular pigments, thus indicating decreased macular cell function and sustained accumulation of oxidative microglial breakdown products [78]. Conversely, near-infrared FAF showed decreased FAF intensity in the macular area, a mosaic foveal pattern, and a cystoid signal [79]. Despite these findings, stricter imaging guidelines are needed to establish the clinical utility of FAF in the context of DME.

3. Functional Retinal Imaging Techniques

3.1. Optical Coherence Tomography Angiography (OCT-A)

OCT-A is a non-invasive functional addition to structural OCT that maps vascular blood flow within all layers of the retina and is used to image the retinal microvasculature and choroid. Motion contrast is detected by the comparison of repeated B-scans on the same area of the retina via light waves, with differences in scans occurring due to erythrocyte movement and blood flow. In the end, these repeated scans are used to reconstruct a 3-D structure of retinal and choroidal blood vessels, and segmentation is used to delineate blood vessels into their respective vascular layer [80,81].

There are several benefits to utilizing OCT-A. OCT-A provides a quantitative measure for retinal vasculature and vascular pathology (Figure 6), such as neovascularization, while localizing the depth of the defect. Additionally, OCT-A is capable of visualizing retinal microvessels with high-depth resolution and contrast due to a lack of hyperfluorescence from contrast dye leakage, as in FA [82]. In cases where FA is contraindicated, such as during pregnancy or in patients with a history of anaphylactic reactions to fluorescein, OCT-A provides functional imaging without the need for administration of exogenous contrast agents [83]. Finally, OCT-A can be performed relatively quickly in comparison to FA and indocyanine green angiography (ICGA). Conversely, OCT-A has some limitations; it requires longer imaging times compared to SD-OCT since A-scans occur in the same position of the retina repeatedly. OCT-A also has a small field of view and cannot display alterations in vascular permeability or leakage. Finally, OCT-A is significantly affected by movement, which makes image artifacts more likely to occur [80,82].

Though FA and OCT have classically been used for the identification and monitoring of DME, OCT-A also provides diagnostic potential. The characteristic image findings in DME eyes, when compared to diabetic eyes without DME, are a significantly higher amount of microaneurysms, higher amount of intraretinal microvascular abnormalities (IRMA), broader foveal avascular zone (FAZ), greater capillary non-perfusion, and lower capillary vascular density (CVD) in the deep capillary plexus. The number of microaneurysms is directly correlated to the severity of DME, with the deep capillary plexus being more involved than the superficial capillary plexus [84,85]. Additionally, inflammation can be characterized in DME by examining macrophage-like cells (MLCs) in the macular regions.

MLCs and HRF observed on OCT are emerging as important biomarkers in DME, reflecting underlying inflammation and immune activation. MLCs are visualized at the vitreoretinal interface (VRI), particularly near the internal limiting membrane (ILM), using *en face* OCT and swept-source OCT angiography (SS-OCTA; see section on OCTA). These cells are believed to include activated microglia and hyalocytes, both of which originate from the monocyte-macrophage lineage. MLCs appear larger and more morphologically active in DME, suggesting heightened inflammatory activity. MLC density correlates negatively with vessel density in the deep capillary plexus, indicating a link between inflammation and microvascular compromise. These cells may contribute to the breakdown of the inner blood–retinal barrier (iBRB), promoting vascular leakage and edema formation

In patients with DME, the quantity and density of MLCs are significantly higher than in patients without DME [86]. Similar to SD-OCT, HRF can also be used to assess retinal microglia and macrophage activation [36]. While OCT-A provides valuable imaging potential, it fails to differentiate between leaking and non-leaking microaneurysms, with segmentation defects often occurring in edematous maculas [80]. Despite these constraints, OCT-A can be a quality diagnostic tool for DME, especially when combined with structural OCT.

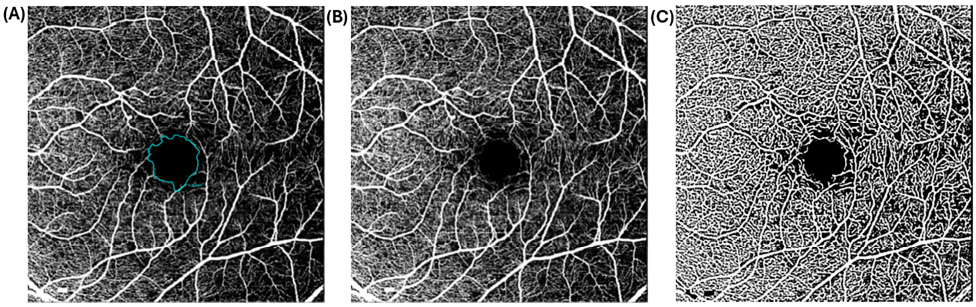


Figure 6. Raw and processed 20 × 20^0 macular-centered OCTA images of a 50-year-old diabetic African American female with moderate NPDR and visual acuity of 0.10 LogMAR. Raw (**A**,**B**) and processed (**C**) OCTA images show areas of capillary non perfusion at the fovea, perifovea, and mid-peripheral retinal regions. The lasso tool for the computation of FAZ area is overlaid onto (**A**). The OCTA images show enlarged FAZ area of 0.75 mm^2 and reduced vessel density. Scale bar: 200 μm.

3.2. Fundus Fluorescein Angiography (FFA)

FFA is a gold-standard yet invasive imaging modality used to visualize retinal and choroidal vasculature, blood flow, and blood vessel leakage caused by endothelial damage, inflammation, and neovascularization, which is commonly seen in DR and DME [87]. FFA and FAF both utilize fluorescence, though FFA requires the intravenous injection of sodium fluorescein, an exogenous agent, into the systemic circulation [87]. Sodium fluorescein is a water-soluble orange dye that binds to plasma proteins in the blood [88]. It absorbs blue light in the range of 465 to 495 nm and emits green light in the range of 520 to 530 nm [87]. Injection of this substance is contraindicated in pregnant patients, patients who exhibit a severe allergic reaction to fluorescein, though moderate allergic reactions can be treated with a corticosteroid or antihistamine, and patients who are at risk for phototoxicity [89,90]. Following the injection of sodium fluorescein, fundus photographs are taken sequentially to capture the fluorescence pattern of the dye as it circulates through the retinal vasculature [87]. Sodium fluorescein lacks the capability to diffuse past the intact retinal pigment epithelium and vascular endothelium, but it diffuses freely in the choriocapillaris [91].

In a normal FFA, there are five phases: the choroidal, arterial, arteriovenous, venous, and recirculation phases. After the dye is injected, it takes ten to fifteen seconds to circulate to the retina. During the choroidal phase, choroidal filling is seen first as the dye initially enters the posterior ciliary arteries. If the cilioretinal artery is present, it will also fill during

the choroidal phase. During the arterial phase, fluorescein dye enters the retinal arteries a couple of seconds after the choroidal phase. The arteriovenous phase occurs a few seconds after the arterial phase, with the dye flowing in a laminar fashion through the precapillary arterioles, capillaries, and postcapillary venules. The venous phase consists of three stages: early, middle, and late. During the early stage, laminar flow occurs through the veins. The middle stage is characterized by complete venous filling. In the late phase, the dye concentration in the arteries is reduced. Finally, in the recirculation phase, the dye is completely emptied from the retinal vasculature, and staining of the optic disc, Bruch's membrane, choroid, and sclera can be visualized [83]. This sequential process provides a comprehensive assessment of retinal circulation. However, despite its exceptional ability to visualize superficial retinal vasculature, FFA lacks the ability to visualize deep capillary networks and the radial peripapillary capillary network [92].

FFA can reveal subtle changes in the retinal vasculature in DR and DME. On FFA imaging, microaneurysms appear as hyperfluorescent punctate areas that correspond with those seen on CFP, which distinguishes them from RPE defects [93,94]. Areas of hypofluorescence indicate capillary non-perfusion and superficial and deep hemorrhages [95]. Hemorrhage hypofluorescent zones are caused by blocked fluorescence. Additionally, macroaneurysm formation is visualized by capillary closure. Diabetic macular ischemia is seen with enlargement of the foveal avascular zone (FAZ). Furthermore, leakage in DME can be graded via FFA as focal or diffuse. Focal leakage originates primarily from microaneurysms, with a circinate ring of hard exudates around the leakage. In contrast, diffuse leakage originates primarily from a generalized breakdown of the BRB from dilated capillaries in the posterior pole. Neovascularization networks leak dye that obscures the view of new vessels. IRMAs, distinguished from neovascularization by their lack of protrusion into the vitreous cavity, can also be visualized in the retina using FAF. The location of these leakage points can be precisely detected on FFA, which can help guide focal laser treatment to the appropriate areas [27,83,95,96].

In recent years, the use of FFA has declined due to the diagnostic utility and non-invasive fundus exams provided by structural OCT and OCT-A [97]. However, wide-field FFA has been increasingly utilized to identify peripheral retinal ischemia, detect neovascularization, and guide panretinal photocoagulation by targeting areas of capillary nonperfusion [98]. Additionally, deep learning models are being developed to convert CFP into FFA images to deliver the benefits of FFA without the need for an invasive procedure [99,100]. This translation also provides valuable diagnostic potential in geographic areas lacking FFA. Overall, FFA is an irreplaceable tool that is complementary to several imaging techniques and provides valuable information regarding retinal vasculature, especially in the context of DR and DME.

4. Conclusions

Understanding the pathological imaging features of DR and DME is critical for early diagnosis and effective management of these retinal diseases. Traditionally, CFPs have been the primary imaging modality for structural imaging of these conditions. However, SD-OCT has emerged as a cornerstone in modern ophthalmic imaging, offering detailed analysis of retinal and choroidal changes, thereby enhancing the assessment of DR and DME progression. Despite the utility of FAF in detecting early structural signs of DR and DME, further research is necessary to correlate imaging findings to disease progression. The advent of new structural imaging technologies, such as UWFI, presents the potential for earlier detection of DR and DME by capturing a broad view of the retina. Furthermore, functional imaging techniques, such as OCT-A and FFA, offer valuable diagnostic infor-

mation via visualization of the retinal microvasculature. These modalities should be used alongside structural imaging techniques to develop a comprehensive clinical picture.

The integration of artificial intelligence and deep learning models into imaging analysis also holds significant promise. These novel technologies can enhance diagnostic accuracy and efficiency and improve access to imaging for patients who face barriers to care. A recent meta-analysis reported that artificial intelligence systems interpreting fundus photographs achieved a sensitivity of 92.6% and a specificity of 91.1%, while OCT-based systems performed slightly better, with a sensitivity of 95.9% and a specificity of 97.9% [101]. A multicenter study developed a deep learning model based on ultrawide-field scanning laser ophthalmoscope images, achieving a specificity of 95.1% for detecting referable diabetic retinopathy and 95.8% for vision-threatening diabetic retinopathy, with corresponding sensitivities of 94.9% and 87.2% [102]. Continued research is essential to advance these technologies, improve their diagnostic utility, and identify new biomarkers for DR and DME. Several imaging biomarkers of interest have already been explored using deep learning models, including automated detection of DRIL, photoreceptor disruption, and HRF on OCT B-scans [103]. Overall, the integration of traditional imaging modalities with emerging biomarkers and novel technologies can enhance the detection and management of DR and DME, thus improving patient outcomes on both an individual and population level.

Author Contributions: Conceptualization, A.M. and M.B.G.; resources, M.B.G. and E.A.; data curation, A.M., E.A. and M.B.G.; writing—original draft preparation, A.M.; writing—review and editing, E.A. and M.B.G.; visualization, A.M. and E.A.; supervision, M.B.G. All authors have read and agreed to the published version of the manuscript.

Funding: This research received no external funding.

Institutional Review Board Statement: Not applicable.

Informed Consent Statement: Not applicable.

Data Availability Statement: The original contributions presented in this study are included in the article. Further inquiries can be directed to the corresponding author(s).

Acknowledgments: This study was supported by ARVO Genentech Career Development Award; University of Alabama at Birmingham (UAB) Integrative Center for Aging Research Pilot Grant, UAB Diabetes Research Center Pilot Grant, UAB Alzheimer's Disease Research Center Pilot Grant, and NIH/NIA R21AG079794 to E. Arthur and the NIH R01EY012601, R01EY028858, R01EY028037, R01EY025383, R01EY032753, R01EY033620, and R01EY034133 to M.B. Grant.

Conflicts of Interest: The authors declare no conflicts of interest.

Abbreviations

The following abbreviations are used in this manuscript:

DM	Diabetes mellitus
DR	Diabetic retinopathy
DME	Diabetic macular edema
NPDR	Non-proliferative diabetic retinopathy
PDR	Proliferative diabetic retinopathy
SD-OCT	Spectral domain optical coherence tomography
OCT-A	Optical coherence tomography angiography
FA	Fluorescein angiography
CFP	Color fundus photography
FAF	Fundus autofluorescence
DRIL	Disorganization of retinal inner layers
FAZ	Foveal avascular zone

BRB	Blood–retinal barrier
HRF	Hyperreflective foci
logMAR VA	Logarithm of minimal angle of resolution visual acuity
sCD14	Soluble CD14
VEGF	Vascular endothelial growth factor
HCF	Hyperreflective choroidal foci
iBRB	Inner blood–retinal barrier
INL	Inner nuclear layer
OPL	Outer plexiform layer
ONL	Outer nuclear layer
CSFT	Central subfield thickness
CRT	Central retinal thickness
ELM	External limiting membrane
EZ	Ellipsoid zone
IS	Inner photoreceptor segments
OS	Outer photoreceptor segments
VMIA	Vitreomacular interface abnormalities
ERM	Epiretinal membrane
DRSS	Diabetic Retinopathy Severity Scale
ETDRS	Early Treatment Diabetic Retinopathy Study
IRMAs	Intraretinal microvascular abnormalities
UWFI	Ultrawide-field imaging
RPE	Retinal pigment epithelium
SW-FAF	Short-wavelength fundus autofluorescence
REFC	Red emission fluorescent components
GEFC	Green emission fluorescent components
ICGA	Indocyanine green angiography
CVD	Capillary vascular density
MLCs	Macrophage-like cells

References

1. National Diabetes Statistics Report |Diabetes| CDC. Available online: https://www.cdc.gov/diabetes/php/data-research/?CDC_AAref_Val=https://www.cdc.gov/diabetes/data/statistics-report/index.html (accessed on 17 July 2024).
2. Tomic, D.; Shaw, J.E.; Magliano, D.J. The burden and risks of emerging complications of diabetes mellitus. *Nat. Rev. Endocrinol.* **2022**, *18*, 525. [CrossRef]
3. Sayin, N.; Kara, N.; Pekel, G. Ocular complications of diabetes mellitus. *World J. Diabetes* **2015**, *6*, 92. [CrossRef]
4. Lang, G.E. Diabetic macular edema. *Ophthalmologica* **2012**, *227* (Suppl. 1), 21–29. [CrossRef]
5. Steinmetz, J.D.; Bourne, R.R.A.; Briant, P.S.; Flaxman, S.R.; Taylor, H.R.B.; Jonas, J.B.; Abdoli, A.A.; Abrha, W.A.; Abualhasan, A.; Abu-Gharbieh, E.G.; et al. Causes of blindness and vision impairment in 2020 and trends over 30 years, and prevalence of avoidable blindness in relation to VISION 2020: The Right to Sight: An analysis for the Global Burden of Disease Study. *Lancet Glob. Health* **2021**, *9*, e144–e160. [CrossRef] [PubMed]
6. Vashist, P.; Singh, S.; Gupta, N.; Saxena, R. Role of Early Screening for Diabetic Retinopathy in Patients with Diabetes Mellitus: An Overview. *Indian. J. Community Med.* **2011**, *36*, 247. [CrossRef]
7. Horie, S.; Ohno-Matsui, K. Progress of Imaging in Diabetic Retinopathy-From the Past to the Present. *Diagnostics* **2022**, *12*, 1684. [CrossRef] [PubMed]
8. Mishra, C.; Tripathy, K. Fundus Camera. In *Compendium of Biomedical Instrumentation*; John Wiley & Sons: Hoboken, NJ, USA, 2023; pp. 853–856. [CrossRef]
9. Sears, C.M.; Nittala, M.G.; Jayadev, C.; Verhoek, M.; Fleming, A.; Van Hemert, J.; Tsui, I.; Sadda, S.R. Comparison of Subjective Assessment and Precise Quantitative Assessment of Lesion Distribution in Diabetic Retinopathy. *JAMA Ophthalmol.* **2018**, *136*, 365–371. [CrossRef]
10. Grading Diabetic Retinopathy from Stereoscopic Color Fundus Photographs—An Extension of the Modified Airlie House Classification: ETDRS Report Number 10. *Ophthalmology* **2020**, *127*, S99–S119. [CrossRef] [PubMed]
11. Early Treatment Diabetic Retinopathy Study Research Group. Fundus Photographic Risk Factors for Progression of Diabetic Retinopathy: ETDRS Report Number 12. *Ophthalmology* **1991**, *98*, 823–833. [CrossRef]

12. Yang, Z.; Tan, T.E.; Shao, Y.; Wong, T.Y.; Li, X. Classification of diabetic retinopathy: Past, present and future. *Front. Endocrinol.* **2022**, *13*, 1079217. [CrossRef]
13. Wilkinson, C.P.; Ferris, F.L.; Klein, R.E.; Lee, P.P.; Agardh, C.D.; Davis, M.; Dills, D.; Kampik, A.; Pararajasegaram, R.; Verdaguer, J.T. Proposed international clinical diabetic retinopathy and diabetic macular edema disease severity scales. *Ophthalmology* **2003**, *110*, 1677–1682. [CrossRef]
14. Cleland, C. Comparing the International Clinical Diabetic Retinopathy (ICDR) severity scale. *Community Eye Health* **2023**, *36*, 10.
15. Terasaki, H.; Sonoda, S.; Tomita, M.; Sakamoto, T. Recent Advances and Clinical Application of Color Scanning Laser Ophthalmoscope. *J. Clin. Med.* **2021**, *10*, 718. [CrossRef]
16. Aiello, L.P.; Odia, I.; Glassman, A.R.; Melia, M.; Jampol, L.M.; Bressler, N.M.; Kiss, S.; Silva, P.S.; Wykoff, C.C.; Sun, J.K.; et al. Comparison of Early Treatment Diabetic Retinopathy Study Standard 7-Field Imaging With Ultrawide-Field Imaging for Determining Severity of Diabetic Retinopathy. *JAMA Ophthalmol.* **2019**, *137*, 65–73. [CrossRef]
17. Silva, P.S.; Cavallerano, J.D.; Sun, J.K.; Soliman, A.Z.; Aiello, L.M.; Aiello, L.P. Peripheral lesions identified by mydriatic ultrawide field imaging: Distribution and potential impact on diabetic retinopathy severity. *Ophthalmology* **2013**, *120*, 2587–2595. [CrossRef] [PubMed]
18. Price, L.D.; Au, S.; Chong, N.V. Optomap ultrawide field imaging identifies additional retinal abnormalities in patients with diabetic retinopathy. *Clin. Ophthalmol.* **2015**, *9*, 527–531. [CrossRef]
19. Attiku, Y.; Nittala, M.G.; Velaga, S.B.; Ramachandra, C.; Bhat, S.; Solanki, K.; Jayadev, C.; Choudhry, N.; Orr, S.M.A.; Jiang, S.; et al. Comparison of diabetic retinopathy severity grading on ETDRS 7-field versus ultrawide-field assessment. *Eye* **2023**, *37*, 2946–2949. [CrossRef] [PubMed]
20. Nanegrungsunk, O.; Patikulsila, D.; Sadda, S.R. Ophthalmic imaging in diabetic retinopathy: A review. *Clin. Exp. Ophthalmol.* **2022**, *50*, 1082–1096. [CrossRef] [PubMed]
21. Sun, J.K.; Lin, M.M.; Lammer, J.; Prager, S.; Sarangi, R.; Silva, P.S.; Aiello, L.P. Disorganization of the retinal inner layers as a predictor of visual acuity in eyes with center-involved diabetic macular edema. *JAMA Ophthalmol.* **2014**, *132*, 1309–1316. [CrossRef]
22. Das, R.; Spence, G.; Hogg, R.E.; Stevenson, M.; Chakravarthy, U. Disorganization of Inner Retina and Outer Retinal Morphology in Diabetic Macular Edema. *JAMA Ophthalmol.* **2018**, *136*, 202–208. [CrossRef]
23. Joltikov, K.A.; Sesi, C.A.; De Castro, V.M.; Davila, J.R.; Anand, R.; Khan, S.M.; Farbman, N.; Jackson, G.R.; Johnson, C.A.; Gardner, T.W. Disorganization of Retinal Inner Layers (DRIL) and Neuroretinal Dysfunction in Early Diabetic Retinopathy. *Investig. Ophthalmol. Vis. Sci.* **2018**, *59*, 5481. [CrossRef]
24. Nicholson, L.; Ramu, J.; Triantafyllopoulou, I.; Patrao, N.V.; Comyn, O.; Hykin, P.; Sivaprasad, S. Diagnostic accuracy of disorganization of the retinal inner layers in detecting macular capillary non-perfusion in diabetic retinopathy. *Clin. Exp. Ophthalmol.* **2015**, *43*, 735–741. [CrossRef]
25. Midena, E.; Torresin, T.; Schiavon, S.; Danieli, L.; Polo, C.; Pilotto, E.; Midena, G.; Frizziero, L. The Disorganization of Retinal Inner Layers Is Correlated to Müller Cells Impairment in Diabetic Macular Edema: An Imaging and Omics Study. *Int. J. Mol. Sci.* **2023**, *24*, 9607–9618. [CrossRef]
26. Cennamo, G.; Montorio, D.; Fossataro, F.; Fossataro, C.; Tranfa, F. Evaluation of vessel density in disorganization of retinal inner layers after resolved diabetic macular edema using optical coherence tomography angiography. *PLoS ONE* **2021**, *16*, e0244789. [CrossRef] [PubMed]
27. Markan, A.; Agarwal, A.; Arora, A.; Bazgain, K.; Rana, V.; Gupta, V. Novel imaging biomarkers in diabetic retinopathy and diabetic macular edema. *Ther. Adv. Ophthalmol.* **2020**, *12*, 2515841420950513. [CrossRef] [PubMed]
28. Gella, L.; Raman, R.; Rani, P.K.; Sharma, T. Spectral domain optical coherence tomography characteristics in diabetic retinopathy. *Oman J. Ophthalmol.* **2014**, *7*, 126–129. [CrossRef]
29. Vujosevic, S.; Bini, S.; Torresin, T.; Berton, M.; Midena, G.; Parrozzani, R.; Martini, F.; Pucci, P.; Daniele, A.R.; Cavarzeran, F.; et al. Hyperreflective retinal spots in normal and diabetic eyes. *Retina* **2017**, *37*, 1092–1103. [CrossRef] [PubMed]
30. Rübsam, A.; Wernecke, L.; Rau, S.; Pohlmann, D.; Müller, B.; Zeitz, O.; Joussen, A.M. Behavior of SD-OCT Detectable Hyperreflective Foci in Diabetic Macular Edema Patients after Therapy with Anti-VEGF Agents and Dexamethasone Implants. *J. Diabetes Res.* **2021**, *2021*, 8820216. [CrossRef]
31. Sasaki, M.; Kawasaki, R.; Noonan, J.E.; Wong, T.Y.; Lamoureux, E.; Wang, J.J. Quantitative Measurement of Hard Exudates in Patients With Diabetes and Their Associations With Serum Lipid Levels. *Investig. Ophthalmol. Vis. Sci.* **2013**, *54*, 5544–5550. [CrossRef]
32. Toto, L.; Romano, A.; Pavan, M.; Degl'iNnocenti, D.; Olivotto, V.; Formenti, F.; Viggiano, P.; Midena, E.; Mastropasqua, R. A deep learning approach to hard exudates detection and disorganization of retinal inner layers identification on OCT images. *Sci. Rep.* **2024**, *14*, 16652. [CrossRef]

33. Lee, H.; Jang, H.; Choi, Y.A.; Kim, H.C.; Chung, H. Association Between Soluble CD14 in the Aqueous Humor and Hyperreflective Foci on Optical Coherence Tomography in Patients With Diabetic Macular Edema. *Investig. Ophthalmol. Vis. Sci.* **2018**, *59*, 715–721. [CrossRef]
34. Vujosevic, S.; Bini, S.; Midena, G.; Berton, M.; Pilotto, E.; Midena, E. Hyperreflective Intraretinal Spots in Diabetics without and with Nonproliferative Diabetic Retinopathy: An In Vivo Study Using Spectral Domain OCT. *J. Diabetes Res.* **2013**, *2013*, 491835. [CrossRef]
35. Uji, A.; Murakami, T.; Nishijima, K.; Akagi, T.; Horii, T.; Arakawa, N.; Muraoka, Y.; Ellabban, A.A.; Yoshimura, N. Association between hyperreflective foci in the outer retina, status of photoreceptor layer, and visual acuity in diabetic macular edema. *Am. J. Ophthalmol.* **2012**, *153*, 710–717.e1. [CrossRef]
36. Qin, S.; Zhang, C.; Qin, H.; Xie, H.; Luo, D.; Qiu, Q.; Liu, K.; Zhang, J.; Xu, G.; Zhang, J. Hyperreflective Foci and Subretinal Fluid Are Potential Imaging Biomarkers to Evaluate Anti-VEGF Effect in Diabetic Macular Edema. *Front. Physiol.* **2021**, *12*, 791442. [CrossRef]
37. Roy, R.; Saurabh, K.; Shah, D.; Chowdhury, M.; Goel, S. Choroidal Hyperreflective Foci: A Novel Spectral Domain Optical Coherence Tomography Biomarker in Eyes With Diabetic Macular Edema. *Asia Pac J. Ophthalmol.* **2019**, *8*, 314–318. [CrossRef]
38. Saurabh, K.; Roy, R.; Herekar, S.; Mistry, S.; Choudhari, S. Validation of choroidal hyperreflective foci in diabetic macular edema through a retrospective pilot study. *Indian. J. Ophthalmol.* **2021**, *69*, 3203. [CrossRef]
39. Otani, T.; Kishi, S.; Maruyama, Y. Patterns of diabetic macular edema with optical coherence tomography. *Am. J. Ophthalmol.* **1999**, *127*, 688–693. [CrossRef] [PubMed]
40. Spaide, R.F. Retinal Vascular Cystoid Macular Edema: Review and New Theory. *Retina* **2016**, *36*, 1823–1842. [CrossRef] [PubMed]
41. Yanoff, M.; Fine, B.S.; Brucker, A.J.; Eagle, R.C. Pathology of human cystoid macular edema. *Surv. Ophthalmol.* **1984**, *28* (Suppl. 2), 505–511. [CrossRef] [PubMed]
42. Deák, G.G.; Bolz, M.; Ritter, M.; Prager, S.; Benesch, T.; Schmidt-Erfurth, U. A Systematic Correlation between Morphology and Functional Alterations in Diabetic Macular Edema. *Investig. Ophthalmol. Vis. Sci.* **2010**, *51*, 6710–6714. [CrossRef]
43. Yalçın, N.G.; Özdek, Ş. The Relationship Between Macular Cyst Formation and Ischemia in Diabetic Macular Edema. *Turk. J. Ophthalmol.* **2019**, *49*, 194. [CrossRef]
44. Murakami, T.; Nishijima, K.; Akagi, T.; Uji, A.; Horii, T.; Ueda-Arakawa, N.; Muraoka, Y.; Yoshimura, N. Optical Coherence Tomographic Reflectivity of Photoreceptors beneath Cystoid Spaces in Diabetic Macular Edema. *Investig. Ophthalmol. Vis. Sci.* **2012**, *53*, 1506–1511. [CrossRef]
45. Sanchez-Tocino, H.; Alvarez-Vidal, A.; Maldonado, M.J.; Moreno-Montanes, J.; Garcia-Layana, A. Retinal thickness study with optical coherence tomography in patients with diabetes. *Investig. Ophthalmol. Vis. Sci.* **2002**, *43*, 1588–1594.
46. Torjani, A.; Mahmoudzadeh, R.; Salabati, M.; Cai, L.; Hsu, J.; Garg, S.; Ho, A.C.; Yonekawa, Y.; Kuriyan, A.E.; Starr, M.R. Factors Associated with Fluctuations in Central Subfield Thickness in Patients with Diabetic Macular Edema Using Diabetic Retinopathy Clinical Research Protocols T and V. *Ophthalmol. Sci.* **2023**, *3*, 100226. [CrossRef]
47. Buabbud, J.C.; Al-Latayfeh, M.M.; Sun, J.K. Optical coherence tomography imaging for diabetic retinopathy and macular edema. *Curr. Diabetes Rep.* **2010**, *10*, 264–269. [CrossRef] [PubMed]
48. Diabetic Retinopathy Clinical Research Network; Browning, D.J.; Glassman, A.R.; Aiello, L.P.; Beck, R.W.; Brown, D.M.; Fong, D.S.; Bressler, N.M.; Danis, R.P.; Kinyoun, J.L.; et al. Relationship between optical coherence tomography-measured central retinal thickness and visual acuity in diabetic macular edema. *Ophthalmology* **2007**, *114*, 525–536. [CrossRef]
49. Marolo, P.; Borrelli, E.; Gelormini, F.; Boscia, G.; Parisi, G.; Fallico, M.; Barresi, C.; Lari, G.; Berni, A.; Bandello, F.; et al. Retinal Thickness Deviation: A New OCT Parameter for Assessing Diabetic Macular Edema. *J. Clin. Med.* **2023**, *12*, 3976. [CrossRef] [PubMed]
50. You, Q.S.; Tsuboi, K.; Guo, Y.; Wang, J.; Flaxel, C.J.; Bailey, S.T.; Huang, D.; Jia, Y.; Hwang, T.S. Comparison of Central Macular Fluid Volume With Central Subfield Thickness in Patients with Diabetic Macular Edema Using Optical Coherence Tomography Angiography. *JAMA Ophthalmol.* **2021**, *139*, 734–741. [CrossRef]
51. Tsuboi, K.; You, Q.S.; Guo, Y.; Wang, J.; Flaxel, C.J.; Bailey, S.T.; Huang, D.; Jia, Y.; Hwang, T.S. Automated Macular Fluid Volume As a Treatment Indicator for Diabetic Macular Edema. *J. Vitreoretin. Dis.* **2023**, *7*, 226–231. [CrossRef] [PubMed]
52. Starr, M.R.; Salabati, M.; Mahmoudzadeh, R.; Patel, L.G.; Ammar, M.J.; Hsu, J.; Garg, S.; Ho, A.C.; Kuriyan, A.E. Fluctuations in Central Subfield Thickness Associated With Worse Visual Outcomes in Patients With Diabetic Macular Edema in Clinical Trial Setting. *Am. J. Ophthalmol.* **2021**, *232*, 90–97. [CrossRef]
53. Pelosini, L.; Hull, C.C.; Boyce, J.F.; McHugh, D.; Stanford, M.R.; Marshall, J. Optical coherence tomography may be used to predict visual acuity in patients with macular edema. *Investig. Ophthalmol. Vis. Sci.* **2011**, *52*, 2741–2748. [CrossRef]
54. Spaide, R.F.; Curcio, C.A. Anatomical correlates to the bands seen in the outer retina by optical coherence tomography: Literature review and model. *Retina* **2011**, *31*, 1609–1619. [CrossRef]
55. Staurenghi, G.; Sadda, S.; Chakravarthy, U.; Spaide, R.F. Proposed lexicon for anatomic landmarks in normal posterior segment spectral-domain optical coherence tomography: The IN•OCT consensus. *Ophthalmology* **2014**, *121*, 1572–1578. [CrossRef]

56. Murakami, T.; Felinski, E.A.; Antonetti, D.A. Occludin Phosphorylation and Ubiquitination Regulate Tight Junction Trafficking and Vascular Endothelial Growth Factor-induced Permeability. *J. Biol. Chem.* **2009**, *284*, 21036. [CrossRef]
57. Lee, K.E.; Heitkotter, H.; Carroll, J. Challenges Associated with Ellipsoid Zone Intensity Measurements Using Optical Coherence Tomography. *Transl. Vis. Sci. Technol.* **2021**, *10*, 27. [CrossRef] [PubMed]
58. Jain, A.; Saxena, S.; Khanna, V.K.; Shukla, R.K.; Meyer, C.H. Status of serum VEGF and ICAM-1 and its association with external limiting membrane and inner segment-outer segment junction disruption in type 2 diabetes mellitus. *Mol. Vis.* **2013**, *19*, 1760. [PubMed]
59. Saxena, S.; Sadda, S.V.R. Focus on external limiting membrane and ellipsoid zone in diabetic macular edema. *Indian. J. Ophthalmol.* **2021**, *69*, 2925. [CrossRef]
60. Maheshwary, A.S.; Oster, S.F.; Yuson, R.M.S.; Cheng, L.; Mojana, F.; Freeman, W.R. The association between percent disruption of the photoreceptor inner segment-outer segment junction and visual acuity in diabetic macular edema. *Am. J. Ophthalmol.* **2010**, *150*, 63–67.e1. [CrossRef]
61. Akbar Khan, I.; Mohamed, M.D.; Mann, S.S.; Hysi, P.G.; Laidlaw, D.A. Prevalence of vitreomacular interface abnormalities on spectral domain optical coherence tomography of patients undergoing macular photocoagulation for centre involving diabetic macular oedema. *Br. J. Ophthalmol.* **2015**, *99*, 1078–1081. [CrossRef] [PubMed]
62. Wong, Y.; Steel, D.H.W.; Habib, M.S.; Stubbing-Moore, A.; Bajwa, D.; Avery, P.J.; The Sunderland Eye Infirmary study group. Vitreoretinal interface abnormalities in patients treatedwith ranibizumab for diabetic macular oedema. *Graefe's Arch. Clin. Exp. Ophthalmol.* **2017**, *255*, 733–742. [CrossRef]
63. Chang, C.K.; Cheng, C.K.; Bai, C.H.; Peng, C.H.; Hu, C.C. Development of vitreomacular interface abnormality in patients with diabetic macular edema. *Taiwan J. Ophthalmol.* **2012**, *2*, 93–98. [CrossRef]
64. Mikhail, M.; Stewart, S.; Seow, F.; Hogg, R.; Lois, N. Vitreomacular interface abnormalities in patients with diabetic macular oedema and their implications on the response to anti-VEGF therapy. *Graefe's Arch. Clin. Exp. Ophthalmol.* **2018**, *256*, 1411. [CrossRef]
65. Lewis, H.; Abrams, G.W.; Blumenkranz, M.S.; Campo, R.V. Vitrectomy for diabetic macular traction and edema associated with posterior hyaloidal traction. *Ophthalmology* **1992**, *99*, 753–759. [CrossRef]
66. Kulikov, A.N.; Sosnovskii, S.V.; Berezin, R.D.; Maltsev, D.S.; Oskanov, D.H.; Gribanov, N.A. Vitreoretinal interface abnormalities in diabetic macular edema and effectiveness of anti-VEGF therapy: An optical coherence tomography study. *Clin. Ophthalmol.* **2017**, *11*, 1995–2002. [CrossRef]
67. Croce, A.C.; Bottiroli, G. Autofluorescence Spectroscopy and Imaging: A Tool for Biomedical Research and Diagnosis. *Eur. J. Histochem.* **2014**, *58*, 320–337. [CrossRef]
68. Calvo-Maroto, A.M.; Cerviño, A. Spotlight on fundus autofluorescence. *Clin. Optom.* **2018**, *10*, 25. [CrossRef] [PubMed]
69. Călin, E.F.; Popescu, S.I.P.; Cernat, C.C.C.; Patoni, C.; Popescu, M.N.; Mușat, O. Lipofuscin: A key compound in ophthalmic practice. *Rom. J. Ophthalmol.* **2021**, *65*, 109–113. [CrossRef] [PubMed]
70. Durrani, K.; Foster, C.S. Fundus autofluorescence imaging in posterior uveitis. *Semin. Ophthalmol.* **2012**, *27*, 228–235. [CrossRef] [PubMed]
71. Rovati, L.; Docchio, F. Autofluorescence methods in ophthalmology. *J. Biomed. Opt.* **2004**, *9*, 9. [CrossRef]
72. Shi, D.; Zhang, W.; He, S.; Chen, Y.; Song, F.; Liu, S.; Wang, R.; Zheng, Y.; He, M. Translation of Color Fundus Photography into Fluorescein Angiography Using Deep Learning for Enhanced Diabetic Retinopathy Screening. *Ophthalmol. Sci.* **2023**, *3*, 100401. [CrossRef]
73. Vujosevic, S.; Casciano, M.; Pilotto, E.; Boccassini, B.; Varano, M.; Midena, E. Diabetic macular edema: Fundus autofluorescence and functional correlations. *Investig. Ophthalmol. Vis. Sci.* **2011**, *52*, 442–448. [CrossRef] [PubMed]
74. Bindewald, A.; Bird, A.C.; Dandekar, S.S.; Dolar-Szczasny, J.; Dreyhaupt, J.; Fitzke, F.W.; Einbock, W.; Holz, F.G.; Jorzik, J.J.; Keilhauer, C.; et al. Classification of Fundus Autofluorescence Patterns in Early Age-Related Macular Disease. *Investig. Ophthalmol. Vis. Sci.* **2005**, *46*, 3309–3314. [CrossRef]
75. Winkler, B.S.; Boulton, M.E.; Gottsch, J.D.; Sternberg, P. Oxidative damage and age-related macular degeneration. *Mol. Vis.* **1999**, *5*, 32. [PubMed] [PubMed Central]
76. Xu, H.; Chen, M.; Manivannan, A.; Lois, N.; Forrester, J.V. Age-dependent accumulation of lipofuscin in perivascular and subretinal microglia in experimental mice. *Aging Cell.* **2008**, *7*, 58–68. [CrossRef] [PubMed]
77. Waldstein, S.M.; Hickey, D.; Mahmud, I.; Kiire, C.A.; Charbel Issa, P.; Chong, N.V. Two-wavelength fundus autofluorescence and macular pigment optical density imaging in diabetic macular oedema. *Eye* **2012**, *26*, 1078–1085. [CrossRef]
78. Vujosevic, S.; Toma, C.; Nucci, P.; Brambilla, M.; De Cillà, S. Quantitative Color Fundus Autofluorescence in Patients with Diabetes Mellitus. *J. Clin. Med.* **2021**, *10*, 48. [CrossRef]
79. Calvo-Maroto, A.M.; Esteve-Taboada, J.J.; Pérez-Cambrodí, R.J.; Madrid-Costa, D.; Cerviño, A. Pilot Study on Visual Function and Fundus Autofluorescence Assessment in Diabetic Patients. *J. Ophthalmol.* **2016**, *2016*, 1287847. [CrossRef]

80. Chung, H.; Park, B.; Shin, H.J.; Kim, H.C. Correlation of fundus autofluorescence with spectral-domain optical coherence tomography and vision in diabetic macular edema. *Ophthalmology* **2012**, *119*, 1056–1065. [CrossRef]
81. Yoshitake, S.; Murakami, T.; Horii, T.; Uji, A.; Ogino, K.; Unoki, N.; Nishijima, K.; Yoshimura, N. Qualitative and quantitative characteristics of near-infrared autofluorescence in diabetic macular edema. *Ophthalmology* **2014**, *121*, 1036–1044. [CrossRef]
82. Spaide, R.F.; Fujimoto, J.G.; Waheed, N.K.; Sadda, S.R.; Staurenghi, G. Optical coherence tomography angiography. *Prog. Retin. Eye Res.* **2018**, *64*, 1–55. [CrossRef]
83. Nouri, H.; Abtahi, S.H.; Mazloumi, M.; Samadikhadem, S.; Arevalo, J.F.; Ahmadieh, H. Optical coherence tomography angiography in diabetic retinopathy: A major review. *Surv. Ophthalmol.* **2024**, *69*, 558–574. [CrossRef]
84. De Oliveira, P.R.C.; Berger, A.R.; Chow, D.R. Optical coherence tomography angiography in chorioretinal disorders. *Can. J. Ophthalmol.* **2017**, *52*, 125–136. [CrossRef]
85. Ricardi, F.; Reibaldi, M.; Bandello, F.; Borrelli, E. Fluorescein Angiography. In *Retinal and Choroidal Vascular Diseases of the Eye*; Academic Press: Cambridge, MA, USA, 2023; pp. 71–79. [CrossRef]
86. Braham, I.Z.; Kaouel, H.; Boukari, M.; Ammous, I.; Errais, K.; Boussen, I.M.; Zhioua, R. Optical coherence tomography angiography analysis of microvascular abnormalities and vessel density in treatment-naïve eyes with diabetic macular edema. *BMC Ophthalmol.* **2022**, *22*, 418. [CrossRef]
87. Mirshahi, R.; Riazi-Esfahani, H.; Pour, E.K.; Fadakar, K.; Yarmohamadi, P.; Alemzadeh, S.A.; Chaibakhsh, S.; Falavarjani, K.G. Differentiating features of OCT angiography in diabetic macular edema. *Sci. Rep.* **2021**, *11*, 23398. [CrossRef] [PubMed]
88. Wang, Z.; An, H.; Tang, J.; Jin, E.; Li, S.; Zhang, L.; Huang, L.; Qu, J. Elevated number and density of macrophage-like cell as a novel inflammation biomarker in diabetic macular edema. *Sci. Rep.* **2023**, *13*, 5320. [CrossRef] [PubMed]
89. Littlewood, R.; Mollan, S.P.; Pepper, I.M.; Hickman, S.J. The Utility of Fundus Fluorescein Angiography in Neuro-Ophthalmology. *Neuro-Ophthalmol.* **2019**, *43*, 217. [CrossRef] [PubMed]
90. O'goshi, K.I.; Serup, J. Safety of sodium fluorescein for in vivo study of skin. *Skin. Res. Technol.* **2006**, *12*, 155–161. [CrossRef]
91. Kornblau, I.S.; El-Annan, J.F. Adverse reactions to fluorescein angiography: A comprehensive review of the literature. *Surv. Ophthalmol.* **2019**, *64*, 679–693. [CrossRef]
92. Balny, C.; Douzou, P. Production of superoxide ions by photosensitization of dyes. *Biochem. Biophys. Res. Commun.* **1974**, *56*, 386–391. [CrossRef]
93. Grayson, M.C.; Laties, A.M. Ocular Localization of Sodium Fluorescein: Effects of Administration in Rabbit and Monkey. *Arch. Ophthalmol.* **1971**, *85*, 600–609. [CrossRef]
94. Spaide, R.F.; Klancnik, J.M.; Cooney, M.J. Retinal vascular layers imaged by fluorescein angiography and optical coherence tomography angiography. *JAMA Ophthalmol.* **2015**, *133*, 45–50. [CrossRef] [PubMed]
95. Norton, E.W.; Gutman, F. Diabetic retinopathy studied by fluorescein angiography. *Trans. Am. Ophthalmol. Soc.* **1965**, *63*, 108. Available online: https://www.ncbi.nlm.nih.gov/pmc/articles/PMC1310188/ (accessed on 25 July 2024). [CrossRef] [PubMed]
96. Salz, D.A.; Witkin, A.J. Imaging in diabetic retinopathy. *Middle East Afr. J. Ophthalmol.* **2015**, *22*, 145–150. [CrossRef]
97. Rasta, S.H.; Nikfarjam, S.; Javadzadeh, A. Detection of retinal capillary nonperfusion in fundus fluorescein angiogram of diabetic retinopathy. *Bioimpacts* **2015**, *5*, 183. [CrossRef] [PubMed]
98. Ong, J.X.; Nesper, P.L.; Fawzi, A.A.; Wang, J.M.; Lavine, J.A. Macrophage-Like Cell Density Is Increased in Proliferative Diabetic Retinopathy Characterized by Optical Coherence Tomography Angiography. *Investig. Ophthalmol. Vis. Sci.* **2021**, *62*, 2. [CrossRef] [PubMed] [PubMed Central]
99. Early Treatment Diabetic Retinopathy Study Research Group. Fluorescein Angiographic Risk Factors for Progression of Diabetic Retinopathy: ETDRS Report Number 13. *Ophthalmology* **1991**, *98*, 834–840. [CrossRef]
100. Shen, X.; Zhou, T.; Sun, Z.; Zheng, Y.; Lin, B.; Huang, Y. Trends in application of fundus fluorescein angiography in fundus diseases during a recent ten-year period. *Photodiagn. Photodyn. Ther.* **2024**, *46*, 104029. [CrossRef]
101. Lam, C.; Wong, Y.L.; Tang, Z.; Hu, X.; Nguyen, T.X.; Yang, D.; Zhang, S.; Ding, J.; Szeto, S.K.H.; Ran, A.R.; et al. Performance of Artificial Intelligence in Detecting Diabetic Macular Edema From Fundus Photography and Optical Coherence Tomography Images: A Systematic Review and Meta-analysis. *Diabetes Car.* **2024**, *47*, 304–319. [CrossRef] [PubMed]
102. Tang, F.; Luenam, P.; Ran, A.R.; Quadeer, A.A.; Raman, R.; Sen, P.; Khan, R.; Giridhar, A.; Haridas, S.; Iglicki, M.; et al. Detection of Diabetic Retinopathy from Ultra-Widefield Scanning Laser Ophthalmoscope Images: A Multicenter Deep Learning Analysis. *Ophthalmol. Retina* **2021**, *5*, 1097–1106. [CrossRef] [PubMed]
103. Yao, J.; Lim, J.; Lim, G.Y.S.; Ong, J.C.L.; Ke, Y.; Tan, T.F.; Tan, T.E.; Vujosevic, S.; Ting, D.S.W. Novel artificial intelligence algorithms for diabetic retinopathy and diabetic macular edema. *Eye Vis.* **2024**, *11*, 23. [CrossRef] [PubMed] [PubMed Central]

Disclaimer/Publisher's Note: The statements, opinions and data contained in all publications are solely those of the individual author(s) and contributor(s) and not of MDPI and/or the editor(s). MDPI and/or the editor(s) disclaim responsibility for any injury to people or property resulting from any ideas, methods, instructions or products referred to in the content.